Insights from scanning tunneling microscopy experiments into correlated electron systems

Benschop, T.

Chapter 4

Amplifier for scanning tunneling microscopy at MHz frequencies

Conventional scanning tunneling microscopy (STM) is limited to a bandwidth of a few kHz around DC. Here, we develop, build, and test a novel amplifier circuit capable of measuring the tunneling current in the MHz regime while simultaneously performing conventional STM measurements. This is achieved with an amplifier circuit including a LC tank with a quality factor exceeding 600 and a home-built, low-noise high electron mobility transistor. The amplifier circuit functions while simultaneously scanning with atomic resolution in the tunneling regime, i.e., at junction resistances in the range of giga-ohms, and down towards point contact spectroscopy. To enable high signal-to-noise ratios and meet all technical requirements for the inclusion in a commercial low temperature, ultra-high vacuum STM, we use superconducting cross-wound inductors and choose materials and circuit elements with low heat load. We demonstrate the high performance of the amplifier by measuring the Poissonian noise of tunneling electrons on an atomically clean Au(111) surface.

This chapter has been published as K.M. Bastiaans, T. Benschop, D. Chatzopoulos, D. Cho, Q. Dong, Y. Jin, and M. P. Allan, Amplifier for scanning tunneling microscopy at MHz frequencies, *Review of Scientific Instruments*, 89(9):093709, 2018

4.1 Introduction

Possible applications of scanning tunneling microscopy (STM) experiments in the MHz regime include high-frequency differential conductance measurements, scanning spin resonance experiments, and noise spectroscopy on the atomic scale. Conventionally, this is prevented in STM by the combination of a GOhm resistance of the tunnel junction and a capacitor from the cabling which together form a low pass filter in the kHz regime. In this chapter, we build a matching circuit including superconducting inductors and a home-built HEMT that allows us to measure STM currents at MHz frequencies while remaining in tunneling and with atomic resolution. We demonstrate the amplifier's superior performance by measuring Poissonian noise of tunneling electrons on a clean Au(111) surface.

We start with an introduction to noise spectroscopy. Measurements of electronic noise can yield information in mesoscopic systems that is not present in their time-averaged transport characteristics, including fractional charges in the quantum hall regime [106, 107], the doubling of charge in Andreev processes [108], Coulomb interactions in quantum dots [109–112] and the vanishing of noise in break junctions at the quantum conductance [113]. Generally, the quantity of interest is the deviation of the noise from the Poissonian noise of independent tunneling events of electrons, $S_P = 2e|I|$, with e the electron charge and I the current [114,115]. Here we define the normalized noise S_n as the ratio between measured (S) and Poissonian (S_P) noise, $S_n = S/S_P$, similar to the Fano factor F. For an uncorrelated electronic liquid, one expects $S_n = 1$; but one can imagine systems where the charge of the carriers is not equal to the electron charge ($q \neq e$) or where the electron flow is strongly correlated. In these cases, the Fano factor will not be equal to unity, i.e. the current noise will be smaller or larger than the Poissonian value even though the time-averaged value of the current will not be influenced. Resolving the noise with atomic precision might provide us with new information in systems with strong electronic correlations or charge aggregations that are not present in the mean current. This is our main motivation to combine noise measurement with scanning probe microscopy.

Bringing noise measurements to STM in the tunneling regime comes with unique challenges, which prevented any atomic resolution noise measurement in the tunneling regime thus far. The high impedance of the tunnel junction, formed by the few angstroms vacuum gap between the STM tip and sample, is the critical obstacle. Together with the capacitance of the interfacing coax cable, the junction acts as a low pass filter only allowing transmission of signals in the small frequency range [116]. Moreover, conventional amplifiers used in STM also have a limited bandwidth due to a large feedback resistor and unavoidable parasitic capacitances [1]. This conventional STM circuitry limits the bandwidth to detect the tunneling current from DC to a few kHz (figure 4.1a). Possible solutions to this are bootstrapping the amplifier [117–120], or impedance matching [116]. These enabled noise measurements in MOhm tunnel junctions [116, 117, 121, 122], but a GOhm impedance as it is present in many STM experiments still leads to prohibitive losses in the matching circuit.

In this chapter, we report on a new amplifier circuit that allows us to overcome these challenges. The requirements for our amplifier were: (i) the amplifier should not interfere with traditional STM measurements, (ii) it should work in the GOhm regime, (iii), it has to be possible to easily implement the amplifier in a commercial STM, (iv) it has to be compatible with UHV, implying low outgassing so that the system can be baked and ultra-high- (cryogenic) vacuum can be achieved.

Our key figures of merit are: (i) the low noise of the circuit, (ii) the most efficient separation of high and low frequency signals, and (iii) the highest possible Q factor of the resonator for highest amplification at 4.3 MHz.

This chapter is structured as follows. Noise in a STM junction is discussed in section 4.2. A block diagram of the newly developed system for noise-spectroscopy measurements in STM is presented in section 4.3.1, followed by a discussion on the requirements for implementing such techniques in STM. Section 4.3.2 describes the realization of this new amplifier. A demonstration measurement on an Au(111) surface is presented in section 4.4.

4.2 Noise sources in STM

We start by considering the types of unwanted noise present in a STM setup: mechanical noise, thermal (Johnson) noise, amplifier noise, and flicker (1/f) noise.

They have distinguishable frequency dependences, as shown in figure 4.1a. First, flicker noise or 1/f noise, which is present in almost all electronic devices. The power spectral density of this low-frequency phenomenon is inversely proportional to the frequency and is related to slow resistance fluctuations modulated by temperature variations. Second, noise induced by mechanical vibrations transferred to the junction, where this mechanical noise is converted to current noise. Both noise sources are usually present in the range from DC to a few kHz, indicated by the blue shaded area in figure 4.1a. This emphasizes that the low frequency regime should be avoided and illustrates the disadvantages of the conventional STM bandwidth.

At higher frequencies, the current fluctuations are dominated by thermal noise and shot noise, both of which are informative about the sample. In principle, both phenomena are frequency independent (white noise), and thus are also present at lower frequencies, where the total noise power is dominated by the other contributions. Thermal (also called Johnson-Nyquist) noise is the thermodynamic electronic noise in any conductor with a finite resistance R; its power spectral density is constant throughout the frequency spectrum, $S = 4k_BT$, where k_B is Boltzmann's constant and T is the temperature. Since thermal noise in a conductor is proportional to the temperature, it can be lowered by reducing the temperature. It can be distinguished from shot noise

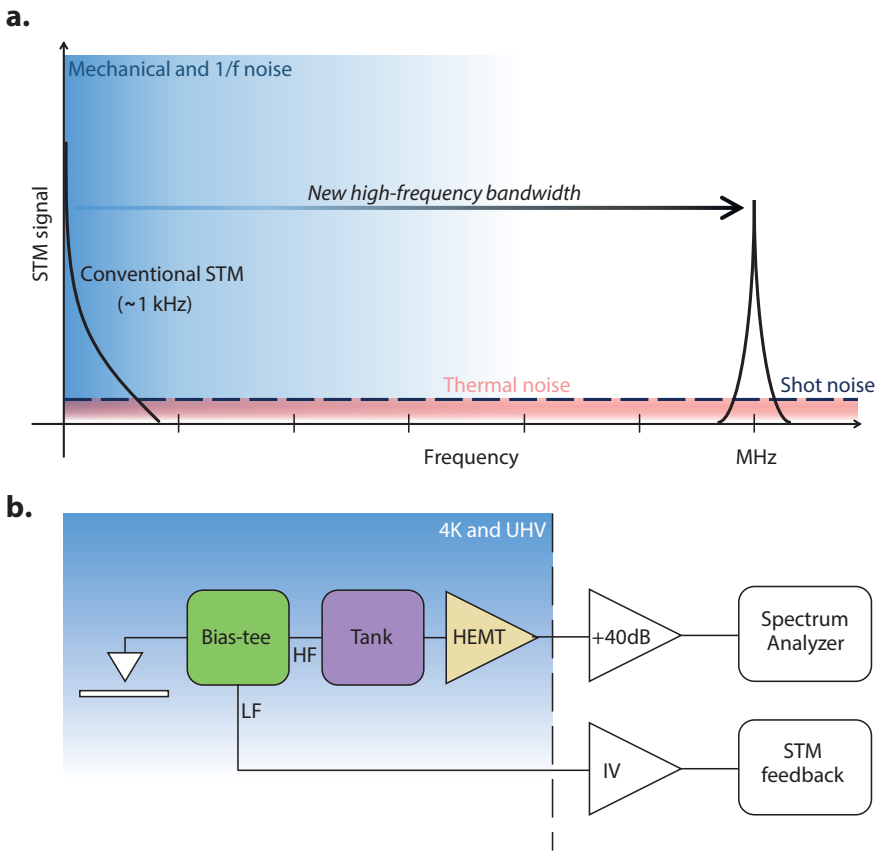

Figure 4.1: Noise in scanning tunneling microscopy (STM)
a) The different noise sources in STM and their frequency dependence are depicted in this schematic plot. At low frequencies mechanical and 1/f noise dominate (indicated by blue region), in this region conventional STM is sensitive. To measure shot noise in the tunnel junction we need to create a new bandwidth at high-frequency. Here thermal noise and shot noise are the most dominant noise sources, since they are independent of frequency. b) Requirements for the newly built amplifier for combining STM and noise-spectroscopy. Crucial components are highlighted: i) the bias-tee (green) that separates the low and high frequency signals. ii) tank circuit (purple). iii) High electron mobility transistor (HEMT, indicated in yellow) to amplify the high-frequency signal. Both the low and high frequency signals have additional room temperature amplification and detection (white).

at zero current, where the latter vanishes.

Our goal is thus to increase the bandwidth and move it to higher frequencies, all whilst retaining the conventional capabilities and staying in the tunneling regime.

4.3 Amplifier and circuit

4.3.1 General idea

To achieve the requirements and goals of section 4.1 while avoiding the unwanted noise sources described in section 4.2, we develop a resonance circuit based amplifier including a resonator-based bias-tee.

We follow the principle of amplifier circuits built for noise spectroscopy measurements in mesoscopic systems [123–126] but we modify it to work for high junction resistances in the GOhm regime and to be compatible with STM. Figure 4.1b shows a block diagram of the amplifier circuit combined with STM. First, a bias-tee (green) separates the low- and high-frequency signals coming from the STM junction. The low-frequency part is needed for the STM feedback loop, where the current is converted to a voltage by a transimpedance amplifier at room temperature. To separate the high frequency, one could use a bias-tee consisting of an inductor in one arm and a capacitor in the other one. However, as we still need a kHz bandwidth in the low frequency branch and as we want to minimize losses of the high frequency signal, we use a resonator based bias-tee.

The high-frequency part of the signal is then passed through the parallel RLC circuit (tank, indicated in purple in figure 4.1b), which converts current to voltage at the resonance frequency of the tank circuit $f_0 = (2\pi\sqrt{LC})^{-1}$. The voltage over the tank circuit is detected by the gate of a high electron mobility transistor (HEMT, indicated in yellow in figure 4.1b) with very low input referred voltage [127, 128] and current noise, operating at the base temperature ($T \sim 4.2$ K in this chapter) of the STM. Through the transimpedance of the HEMT, the voltage fluctuations at its gate are converted into current fluctuations. These are measured over a 50 Ω resistor to finalize the impedance transformation. Note that while the voltage/current gain of the amplifier is of order unity, the gain of power is considerable. A 50 Ω coaxial line connects the amplifier circuit to a commercial 40 dB current amplifier at room temperature. Finally, the signal line is terminated by the 50 Ω input impedance of the spectrum analyzer.

4.3.2 Circuit elements and printed circuit board design

The heart of the circuit is built on a ceramic printed circuit board (Rogers Corp TMM10i, selected for the very low outgassing properties) as depicted in figure 4.3 and

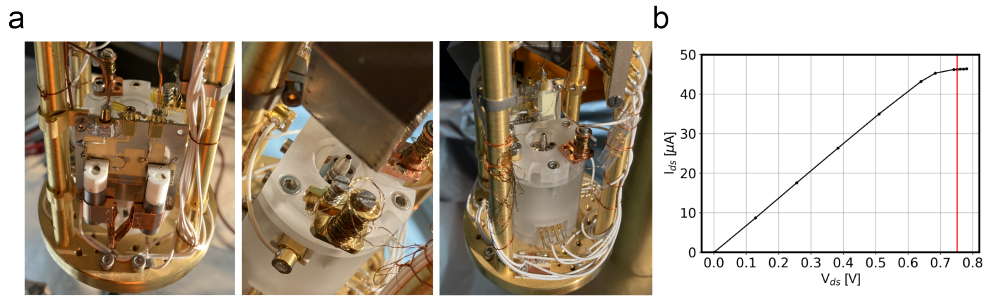

Figure 4.2: Installation in our liquid He 4 system
a) Some photos of our newly built amplifier installed in our STM system. On the left, we see the two shielded niobium inductors that form the resonance circuit, including copper clamps for thermalizing the shields. In the middle, we see the coaxial cable that connects the STM (tip wire) to the input of the amplifier. b) Current-voltage characteristics of the high electron mobility transistor (HEMT) at LHe temperature. The vertical red line indicates our operating point.

described below. Figure 4.3 shows the circuit schematics of the amplifier. The board is located in our home-built liquid He 4 system [129] close to the STM head (figure 4.2a).

The input of the amplifier is connected to the STM tip via a coaxial cable (silver plated Cu mini-coax CW2040-3650F) with a total capacitance between inner and outer conductor of $C_w \approx 16$ pF. This capacitance is including soldered SMP connectors at each end, which actually are the major contributors to this. We purposely made the tip wire as short as possible, to minimize this capacitance, thereby increasing the resonance frequency and quality factor Q of our amplifier. The bias-tee (indicated by green shading) and tank (purple shading) combination is formed by two home-built superconducting Niobium inductors $L_1 \approx 63$ µH, $L_2 \approx 70$ µH coupled by capacitors $C_c = 100$ pF (Murata GRM 0805-size surface mount).

The resonance circuit is formed by the self-resonance of the superconducting Nb inductors in combination with the coaxial cable C_w, providing a resonance frequency of 4.281 MHz. Parallel self-capacitances of the Nb inductors are also shown in figure 4.3, $C_1 \approx C_2 \approx 2$ pF. The Niobium inductors are made by cross-winding annealed Nb wire of 100 μm in diameter around a customized ceramic (macor) core. We choose superconducting Nb inductors to enhance the quality factor of the resonator, increasing current-to-voltage amplification at resonance. The Nb inductors are covered by a Nb shield to minimize Eddy current damping, ensuring the highest possible quality factor Q.

The high-impedance part of the amplification scheme (tank circuit coupled to STM junction) is matched to the 50 Ω impedance of the spectrum analyzer by a home-built low-noise high electron mobility transistor (HEMT) made using molecular beam epitaxy. These specially designed HEMTs have a carrier mobility of 48 m^2/Vs and can

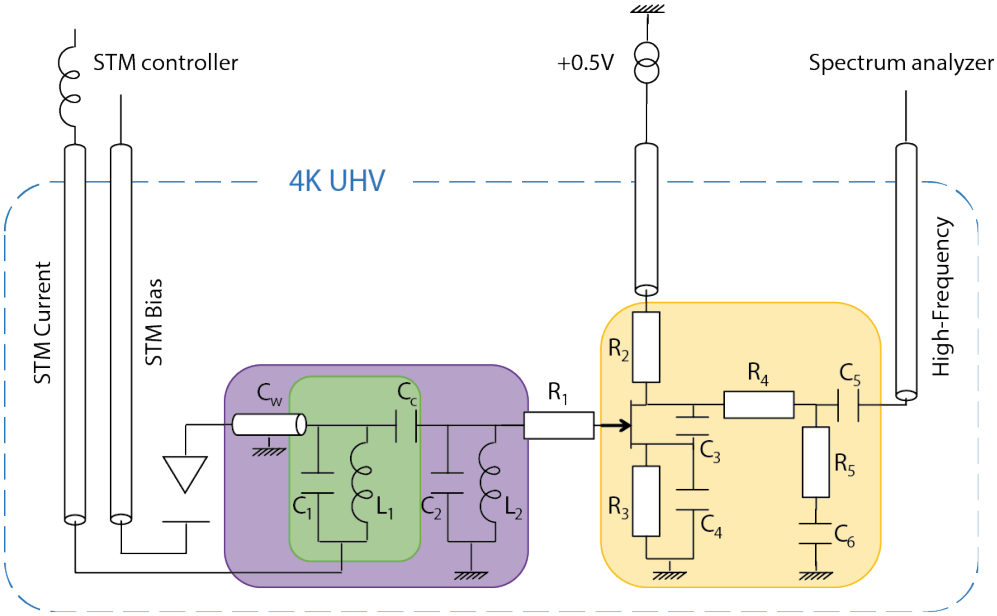

Figure 4.3: Circuit diagram of the newly developed amplifier for scanning noise spectroscopy
The colored boxes (green, purple and yellow) highlight specific parts of the amplifier corresponding to figure 4.1b.

reach unprecedented low noise levels at 1 MHz with a noise voltage of 0.25 nV/$\sqrt{\text{Hz}}$ and a noise current of 2.2 fA/$\sqrt{\text{Hz}}$, under deep cryogenic conditions ($\leq$ 4.2 K), and with an input capacitance of about 5 pF [127, 128]. In addition, components $C_3 = 10$ pF, $R_1 = 10\ \Omega$ and $R_4 = 10\ \Omega$ are placed close to the HEMT case to improve its stability.

The operation point of the HEMT is determined by R_2 and R_3 and the supply voltage. Since we aim to have a very low power dissipation we choose $R_2 = 1$ kΩ and $R_3 = 1.497$ kΩ to give a saturation current of the HEMT of a few tenths of µA while operating at 4 Kelvin. Additionally, the supply voltage is low pass filtered with a simple parallel resistor and capacitor to ground before R_2 (not shown, $R_{filt.} = 51$ kΩ, $C_{filt.} = 39$ nF), in order to reduce incoming noise from the power supply. These components are also installed on the amplifier board at 4 K. A second low pass filter is used at room temperature to further reduce noise from the voltage supply, consisting of a 85 Ω resistor (series) and a 1 µF capacitor (parallel), followed by another 10 kΩ resistor (series). To ensure linear gate voltage to current conversion we operate the HEMT in the saturation regime. We measured the drain current as function of drain-source voltage at 4 K by varying the supply voltage, as depicted in figure 4.2c. In the following demonstration the HEMT is biased in saturation at V = 0.87 V, which

corresponds to a drain-source voltage of $V_{ds} = 0.752$ V (figure 4.2b).

The voltage fluctuations in the 50 Ω line are amplified at room temperature by a +40 dB current amplifier with an input voltage noise of 310 $pV/\sqrt{Hz}$ (Femto HSA-X-1-40) and is finally terminated by the 50 Ω input impedance of a Zurich Instruments MFLI digital spectrum analyzer.

4.4 Noise spectroscopy performance on atomically Au(111)

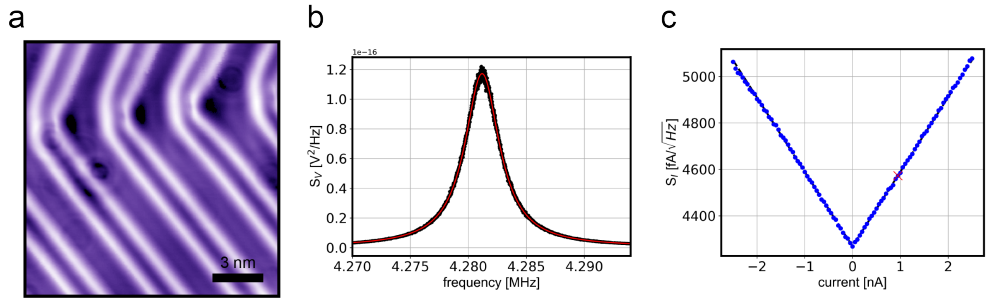

Figure 4.4: Noise measurement results on Au(111)
a) Topography measured on Au(111) surface. A 25 x 25 nm field of view is presented showing the characteristic herringbone reconstruction (setup: V = -250 mV, I = 200 pA). b) Output of the amplifier while the STM is in tunneling (V = 190 mV , I = 950 pA). c) Shot noise as a function of tunneling current measured on the Au(111) surface with a junction resistance of 200 MΩ.

To demonstrate the simultaneous use of the STM feedback system and noise sensitive measurements in the tunneling regime, we performed noise spectroscopy measurements on a gold on mica sample. We believe that the Au(111) surface is most ideal for characterizing our noise-sensitive measurement since the sample is metallic thus any electron correlations are negligible. Figure 4.4a depicts an atomic-resolution image of the Au(111) terminated surface on a 25 nm field of view, where the characteristic 'herringbone' reconstruction is clearly visible.
Figure 4.4b shows the measured output of the high frequency port of the amplifier while electrons are tunneling from tip to sample (I = 950 pA), in a junction of 200 MΩ. We observe a clear resonance peak around 4.281 MHz (black dots) with a Q factor of approximately 1196. The red line shown in the figure is a fit of the circuit transfer function to the data (black). All components here were fixed, except for the capacitance and resistance in the tank. By sweeping the bias of the junction while retaining a constant junction resistance, we can measure the shot noise as a function of the current (figure 4.4c). The spectrum shown in 4.4b corresponds to the datapoint

indicated by the red cross in 4.4c. The clear linear relation between tunneling current and the measured shot noise demonstrates that our amplifier works nicely. From the slope, we find that our amplifier has a power gain of 0.1537.

4.5 Conclusions and outlook

In this chapter we have shown how we have built a low temperature, low noise amplifier to measure the current (fluctuations) in a STM setup at a MHz frequency. We used two superconducting Nb inductors to form a bias-tee and tank resonator coupled to a home-built, low-noise HEMT which is essential for the impedance matching to 50 Ω coax cable. We demonstrated the performance of this amplifier by performing noise spectroscopy measurements on an Au(111) surface.

The development of this MHz amplifier, along with recent developments from other research groups [130], directly opens new paths to explore many-body correlation effects in quantum materials. Further, the developments presented in this chapter also open additional possibilities to probe electron spin resonances (ESR) in STM. ESR often leads to periodic processes and equilibration times in the MHz to GHz regime [131, 132]. These can be measured impedance matched with the presented amplifier instead of measuring indirect effects on the DC current. This could be further improved by guiding the microwave signal directly on the tip with coplanar waveguides, as suggested recently [133]. Finally, one could imagine that the thermal noise, introduced here as an unwanted noise source, could yield information about the sample via cross-correlation noise [134].